

THE MAGAZINE FOR THE METAL ADDITIVE MANUFACTURING INDUSTRY

METAL AM

Vol. 4 No. 4 WINTER 2018



in this issue

**HIGH-VOLUME BINDER JETTING
STANDARDISED X-RAY CT
FORMNEXT 2018 REPORTS**

Sample name	Virgin powder	Controlled contamination		Possible contamination source
		Type	Quantity [wt. %]	
MS1_Ti64	MS1	Ti64	0.5	Contamination through sieving equipment, tools, gloves or AM machine that are previously used with Ti64
MS1_Oxi	MS1	TiO ₂ , Al ₂ O ₃	< 0.5	Production batch with titanium oxide and aluminium oxide inclusions
Ti64_MS1	Ti64	MS1	0.5	Breakage of the steel recoater blade or contamination from AM machine
Ti64_ZrO ₂	Ti64	ZrO ₂	0.5	Breakage of ceramic recoater blade

Table 4 Type and amount of controlled cross-contamination [2]

contamination was that of tungsten particles found within Ti-6Al-4V. These contamination instances are a similar size to those of the bulk material and so an analogous tungsten alloy powder of size range < 75 µm was mixed into 40 g of Ti-6Al-4V powder in a split sample arrangement. Such samples were scanned in a set-up that produced a 22.5 µm voxel size. Contamination occurrences were identified by eye and, for each, a Region Of Interest (ROI) volume was selected manually. The volume was then extracted for size analysis. This manual analysis could be automated; however threshold levels need to be developed and so, for the reported study, manual analysis was used. The extracted volumes were then compared to the associated size fraction of the tungsten powder to assess applicability of the use of large scale samples in this system. The measured size of contaminant, in fact, correlated well with the sieved size fraction of powder and therefore this set-up shows promise for the identification of tungsten contamination in Ti-6Al-4V in a large sample sizes with regard to contaminant size analysis.

The authors' overall conclusion was that the proposed contamination assessment framework should be developed in order to perform cleanliness assessments of metal powder. A holistic approach, using various measurement technologies, must be applied to perform a full assessment of metal powder cleanliness, due to the variety of contamination sources, measurement sample sizes and detection limits.

The demonstrated technologies that currently show promise for cleanliness assessment are optical microscopy, SEM-EDS, DIA and XCT. Cleanliness severity levels for each contamination type, alloy and component end-use sector must be developed within the wider scientific and industrial community.

Development of a reliable method for contamination detection in raw metal powders for AM

A second paper continued on the theme of contamination detection in raw metal powders for Powder Bed Fusion (PBF) AM. This paper came from an Italian academic consortium comprising Eleonora Santecchia, Paolo Mengucci and Gianni Barucca (Universita Politecnica delle Marche), Andrea Gatto, Elena Bassoli and Lucia Denti (Universita di Modena e Reggio Emilia) and Federica Bondoli (Universita di Parma) [2].

Currently, major technical limitations for metal AM relate to the lack of specific qualification standards for AM parts and feedstock materials. Raw powders for Additive Manufacturing are subjected to potential contamination through the full supply chain, from production to the storage and usage (AM) steps. In the reported study, the challenge of cross-contamination detection in feedstock powder materials was addressed. Various scenarios of contaminants and contamination sources during the production and sintering

processes were taken into account and batches of two powders, having the typical compositions of Ti-6Al-4V (EOS Ti64) alloy and maraging steel (MS1) and containing a controlled cross-contamination, were prepared. The contamination was detected using SEM and EDS techniques and a statistical treatment of the collected data allowed quantification of the cross-contamination.

Controlled contamination was introduced to the powder samples following assumptions concerning damage to the PBF equipment (i.e. breaking of the recoater blade), cross-contamination of the powder taking place in the Additive Manufacturing equipment (i.e. the same PBF machine used for different powders) and cross-contamination during powder production or transportation (i.e. sieving equipment, tools or gloves used for different powders). The inspected scenarios are summarised in Table 4.

Scanning electron microscopy observations were performed on a field emission SEM equipped with microanalysis for the energy dispersive spectroscopy (EDS) inspections. Powders were accurately spread and attached on stubs for SEM; three stubs for each cross-contamination condition were characterised.

The chemical compositions of the pure and contaminated powders were checked by collecting three EDS spectra on areas at the same low magnification (200 x), using 20 keV accelerating voltage. Deconvolution of the elemental peaks was used in order to resolve peak overlaps and

	Ni	Co	Mo	Ti	Al	Cr	
MS1	17-19	8.5-9.5	4.5-5.2	0.6-0.8	0.05-0.15	≤ 0.5	
MS1_Ti64	15.4±0.3	10.8±0.1	3.5±0.2	1.50±0.2	0.05±0.01	0.15±0.03	
MS1_Oxi	15.3±0.2	11.2±0.1	3.9±0.2	0.9±0.1	0.06±0.03	0.25±0.06	
	Cu	C	Mn	Si	P	S	Fe
MS1	≤ 0.5	≤ 0.03	≤ 0.1	≤ 0.1	≤ 0.01	≤ 0.01	Bal.
MS1_Ti64	0.14±0.06	-	0.08±0.04	ND	ND	0.06±0.04	Bal.
MS1_Oxi	0.11±0.04	-	ND	ND	ND	ND	Bal.

Table 5 Comparison of elemental concentrations (wt.%) in the MS1 samples (pure and contaminated) [2]

	Al	V	Zr	O	N
Ti64	5.50-6.75	3.50-4.50	-	< 0.20	< 0.05
Ti64_MS1	5.4±0.1	3±0.1	-	ND	ND
Ti64_ZrO ₂	5.6±0.3	3±0.1	0.3±0.1	ND	ND
	C	H	Fe	Y	Ti
Ti64	< 0.08	< 0.015	< 0.30	< 0.005	Bal.
Ti64_MS1	-	ND	ND	ND	Bal.
Ti64_ZrO ₂	-	ND	ND	ND	Bal.

Table 6 Comparison of elemental concentrations (wt.%) in the Ti64 samples (pure and contaminated) [2]

quantitative analysis was performed by the EDS software. In order to ease the detection of the contamination particles, the backscattered electrons (BSE) signal was used together with EDS elemental maps. The low atomic weight of Ti- and Al-based oxides, in the MS1_Oxi samples, resulted in a high BSE contrast and, therefore, contaminant particles in these samples were spotted using SEM-BSE micrographs only.

Quantification of contamination was performed by collecting fifty micrographs for each stub and the elemental map for each position, looking for the major contamination element, i.e., Ti in MS1_Ti64, Fe in Ti64_MS1 and Zr in Ti64_ZrO₂.

The scanning electron microscope working parameters were kept constant for all of the investigations and can be summarised as: (i) 60 µm aperture (beam spot), (ii) 500 x magnification, (iii) 8.3 mm working distance and (iv) 15 keV accelerating voltage.

The latter parameter was chosen in order to achieve an optimised balance between the EDS signal and the BSE contrast/brightness for SEM imaging. The contaminant particles spotted on each micrograph/map were counted and a statistical procedure was then applied, in order to define a calculated contamination. Firstly, the frequency of contaminant particles μ is calculated as in the equation:

$$\mu = \frac{\text{Counted Contaminant Particles}}{\text{Inspected Area}}$$

The total area of the stub is known to be 122.6 mm². The total contaminant particles (TCP) number on the overall stub area is therefore given by:

$$\text{TCP} = (\mu \cdot 122.6)$$

Therefore, the calculated contamination (CC) is obtained as the ratio between the contaminant particles and the total number of virgin powder particles on the stub:

$$\text{CC} = \text{TCP} / \text{TOT}$$

The nominal compositions, as well as the EDS quantification results of the data acquired from MS1 and Ti64-based powders samples, are reported in Tables 5 and 6, respectively.

With reference to the MS1_Oxi samples, the average concentrations reported in Table 5 show no remarkable variations that could be linked to the TiO₂ and Al₂O₃ contaminations. On the other hand, the average Ti concentration in the MS1_Ti64 samples is higher compared with the nominal and MS1_Oxi values, suggesting higher concentrations of titanium.

The vanadium concentrations in Table 6 are below the nominal values in all the samples. Despite the same amount (wt.%) of contamination in the Ti64-based samples, no iron was detected or quantified (Table 6) while a clear signal for zirconium, corresponding to 0.3 wt.%, was obtained, as shown in Fig. 4. Here, two representative spectra, collected on areas of the Ti64-based contaminated samples, are reported in the form of de-convoluted peaks with the background already subtracted. While the peak corresponding to the L α characteristic energy of zirconium is excited by the electron beam (Fig. 4(b)), no peaks related to iron are observed in the Ti64_MS1 spectrum (Fig. 4 (a)). A feasible explanation for this result can be achieved by accounting for the density of the contamination particles under consideration, i.e., 8.0-8.1 g/cm³ for MS1 and 5.8 g/cm³ for ZrO₂.

By collecting the elemental map of the major contamination element, namely that with the highest percentage, it is possible to accurately highlight the cross-contamination powder particles. During the first scan, the mapped element is shown on many points of the micrograph, but, when a very high concentration is detected in a certain area, the software uses this information to adjust the detected chemical element amount on the overall frame area.

For the MS1_Oxi samples, the high BSE-signal contrast, given by the very low atomic weight of the contaminant particles, was sufficient to distinguish

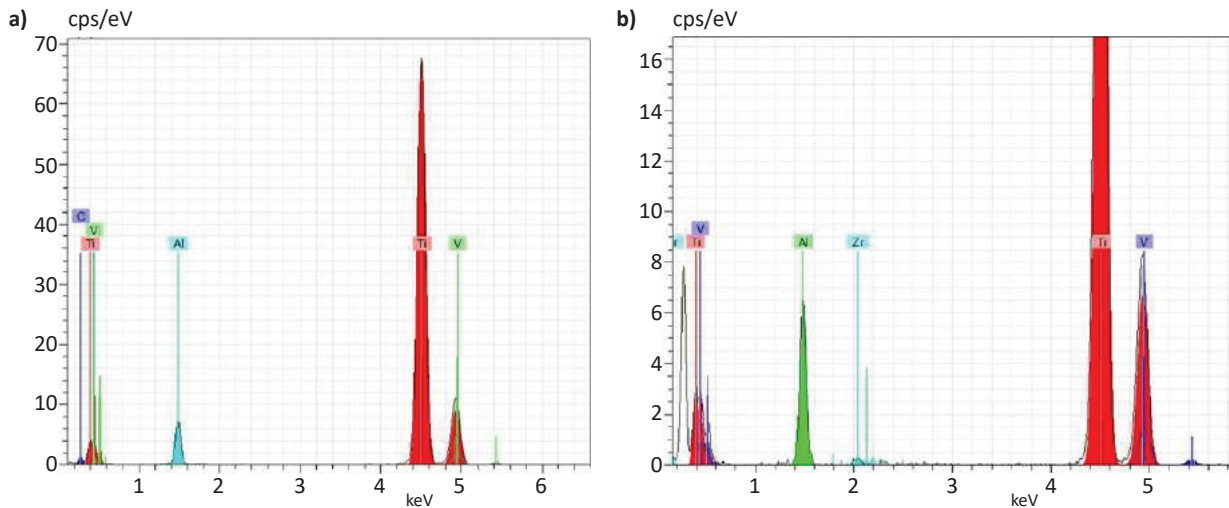


Fig. 4 Representative EDS spectra for the Ti64_MS1 (a) and Ti64_ZrO₂ (b) samples [2]

them from the virgin powders, without the aid of elemental maps. However, the composition of each contaminant particle still needed to be verified using EDS point analysis. The EDS spectrum confirmed that the major elements in the contaminant particles were aluminium, titanium and oxygen. Other unindexed peaks corresponded to Fe, Ni and Mg.

Table 7 shows the average values of calculated contaminations obtained for all the inspected samples. The lowest level of average calculated cross-contamination is given by the samples having an unknown cross-contamination level, or rather MS1_Oxi. Results on specular samples, namely MS1_Ti64 and Ti64_MS1, are of particular interest. The average calculated contamination value of the MS1_Ti64 samples was almost two times higher than that of the Ti64_MS1 samples. Given that the density values of the two virgin

powders correspond to 8.0-8.1 g/cm³ for MS and 4.41 g/cm³ for Ti64, in order to obtain the same amount of 0.5 wt.% of cross-contamination, a lower number (approximately a half) of MS1 particles is required. This explanation also justifies the high level of calculated contamination obtained for the Ti64_ZrO₂ samples, as zirconia has a density equal to 5.81 g/cm³. This larger number of zirconia particles leads to a higher number of nuclei of characteristic X-ray signal generation. This is particularly remarkable for the EDS spectra collected from large areas, or rather those used for the chemical composition quantification (Fig. 4).

A systematic approach for understanding powder influence in powder bed-based AM

The next paper turned the attention to the influence of powder physical characteristics, as opposed to chemical contamination, on processability in powder bed-based Additive Manufacturing. This paper came from Silvia Vock, Solomon Jacobs, Burghardt Kloeden, Thomas Weissgarber and Bernd Kieback (Fraunhofer IFAM, Dresden, Germany) and Michael Haertel (AM Metals GmbH, Germany) [3].

The reported study introduced an approach for the systematic assessment of powder influence along the process chain. As a first step, a database was evaluated in order to identify suitable characterisation techniques and parameters for the reliable and sensitive detection of powder quality changes. In future applications, the continuously growing database would serve as a source for the predictive modelling of process and part properties, based on measured powder characteristics. It was anticipated that this would pave the way for efficient quality control and accelerate the development of process windows for new powder materials.

The authors proposed that powder can be characterised on different levels. On the one hand, the individual particles can be characterised by their morphology, size distribution, composition (main elements and impurities), moisture content on the particle surface and their individual particle density, for instance. On the other hand, physical properties of the powder describe the collective behaviour of the particle assembly, such as the packing of the particles (apparent density, tap density) and the mechanical behaviour of the particle assembly when it is forced to move (flowability). All of these characteristics contribute to a specific process behaviour represented, for

Sample	Average Calculated Contamination (10 ⁻³)
MS1_Ti64	7±1
MS1_Oxi	1.8±0.5
Ti64_MS1	2.7±0.2
Ti64_ZrO ₂	6±2

Table 7 Calculated contamination (CC) values obtained for all of the samples [2]